

## DEPENDENCE OF THE BALQSO FRACTION ON RADIO LUMINOSITY

FRANCESCO SHANKAR, XINYU DAI, AND GREGORY R. SIVAKOFF

*Draft version May 28, 2019*

## ABSTRACT

We find that the fraction of Broad Absorption line quasars (BALQSOs) among the FIRST radio sources in the Sloan Data Release 3, is about  $45.5^{+7.6}_{-7.5}\%$  at the faintest radio powers detected ( $L_{1.4\text{GHz}} \sim 10^{32} \text{ erg s}^{-1}$ ), and rapidly drops to  $23.9^{+3.4}_{-3.1}\%$  at  $L_{1.4\text{GHz}} \sim 3 \times 10^{33} \text{ erg s}^{-1}$ . While the high fraction at low radio power is consistent with the recent near-IR estimate by Dai et al. (2007), the lower fraction at high radio powers is intriguing. The trend is independent of the redshift limits, the optical and radio flux selection limits, the exact definition of a BALQSO, or the exact definition of a radio match. The absorption index decreases with the radio luminosity while the mean maximum wind velocity is roughly a constant at all radio powers. We also find that at fixed optical magnitude, the highest bins of radio luminosity are preferentially populated by non-BALQSOs, consistent with the overall trend. These results are difficult to reconcile with a strictly evolutionary model for the BALQSO and radio emission phases, while a simple geometric model where the apparent radio luminosity function is partly due to beamed, non-BALQSOs can reproduce the results.

*Subject headings:* : black hole physics – galaxies: evolution – galaxies: active – galaxies: jets

## 1. INTRODUCTION

It is a main theme in Active Galactic Nuclei (AGN) studies to understanding various AGN phenomena within coherent schemes. The broad absorption line quasars (BALQSOs) and radio quasars (RQs) are both subsamples of quasars, where BALQSOs exhibit blue-shifted rest-frame ultra-violet absorption troughs (e.g., Weymann et al. 1991) and RQs are characterized by their radio emission (e.g., Matthews & Sandage 1963; Schmidt 1963; Kellermann et al. 1989). The fractions of BALQSOs and RQs are the subjects of many studies (e.g., Weymann et al. 1991; Hewett & Foltz 2003; Ghosh & Punjly 2007). Recently, Dai et al. (2007, DSS hereafter) obtained an intrinsic BALQSO fraction of  $43 \pm 2\%$  using the BALQSOs detected in the Two Micron All Sky Survey (2MASS) and in the Sloan Digital Sky Survey (SDSS) Data Release 3 (DR3) of Trump et al. (2006). Such a fraction is significantly higher than that inferred from optical samples alone, since the BALQSO fraction calculated in the infrared is affected less by the selection effects due to dust extinction and absorption troughs. In Trump et al. (2006), BALQSOs are defined through the Absorption Index (AI), which includes quasars with trough velocities broader than  $1000 \text{ km s}^{-1}$ . This definition is different from the traditional BALQSO Balnicity Index (BI) definition (Weymann et al. 1991) which selects as BALQSOs those sources with trough velocities wider than  $2000 \text{ km s}^{-1}$ . Nevertheless, using the BI definition for BALQSOs, DSS found the intrinsic BALQSO fraction to be  $20 \pm 2\%$ , which is still about double the estimate previously obtained from optical samples with the same selection criteria. On the other hand, recent results on the fraction of RQs in optical samples are between 10–20%, depending on the definition (e.g., Sikora et al. 2007 and references therein). In several studies, the RQ fraction is found to depend on the redshift and optical luminosity (e.g., Jiang et al. 2007).

In general, constraining the intrinsic fractions of BALQSOs and RQs in large, complete quasar samples, is important for understanding the nature of these phenomena such as their ef-

ficiency and/or black hole spin distributions (e.g., Murray et al. 1995; Shankar et al. 2007b; Sikora et al. 2007), and helping constrain AGN and galaxy evolutionary models (e.g., King 2003; Croton et al. 2006; Granato et al. 2006; Hopkins et al. 2006; Lapi et al. 2006, Shankar et al. 2006). The fraction of BALQSOs in RQs is particularly interesting as it may further constrain which quasar sub-samples are caused by geometrical viewing effects and which are caused by evolutionary effects, as well as provide additional clues on the nature and connections between these two apparently disconnected quasar phenomena.

There were no radio BALQSOs detected before the FIRST survey (Stocke et al. 1992). Using the FIRST Bright Quasar Survey, Becker et al. (2000) found 29 BALQSOs, about 14–18% of their total sample, suggesting a frequency of BALQSOs significantly greater than the typical  $\sim 10\%$  inferred from optically selected samples at that time. Within the small sample, they also found that the BALQSO fraction has a complex dependence on radio loudness. Using the Large Bright Quasar Survey, Hewett and Foltz (2003) argued that with a consistent BALQSO definition there is no inconsistency in the BALQSO fractions between optically-selected and radio-selected quasar samples. They also found that “optically-bright BALQSOs are half as likely as non-BALQSOs to be detectable  $S_{1.4\text{GHz}} \gtrsim 1 \text{ mJy}$  as radio sources”. In this paper, we combined the SDSS-DR3 BALQSO sample (Trump et al. 2006) with more than 4,000 BALQSOs with the FIRST survey data (Becker et al. 1995) to study the fraction of BALQSOs in the radio detected sample.

## 2. THE DATA

The parent sample for the Trump et al. (2006) BALQSO catalog is the SDSS DR3 quasar catalog (Schneider et al. 2005). Data were taken in five broad optical bands (*ugriz*) over about  $10,000 \text{ deg}^2$  of the high Galactic latitude sky. The majority of quasars were selected for spectroscopic followup by SDSS based on their optical photometry. In particular, most quasar candidates were selected by their location in the low-redshift ( $z \lesssim 3$ ) *ugri* color cube with its *i*-magnitude limit of 19.1. A sec-

<sup>1</sup> Department of Astronomy, The Ohio State University, Columbus, OH 43210, shankar@astronomy.ohio-state.edu, xinyu@astronomy.ohio-state.edu, sivakoff@astronomy.ohio-state.edu

and higher redshift *griz* color cube was also used with a fainter *i*-magnitude limit of 20.2. Following DSS, we focused on redshift range of  $1.7 \leq z \leq 4.38$ , where BALQSOs are identified by C IV absorption in the SDSS spectra. In the following we present results using both the AI and BI definitions for BALQSOs and show that the main results of this paper do not depend on the adopted definition.

The DR3 quasar catalog also provides the radio flux for those sources which have a counterpart within in the FIRST catalog  $2''$  (Becker et al. 1995). The radio flux densities observed at 1.4 GHz in FIRST were converted from the DR3 catalog AB magnitudes to the specific luminosity emitted at 1.4 GHz,  $L_{1.4\text{GHz}}$ , via the relation

$$L_{1.4\text{GHz}} = \frac{10^{-0.4m_{1.4\text{GHz}}} 3631 \times 10^{-23}}{(1+z)^{1-\alpha}} 4\pi D_L^2 \text{ erg s}^{-1} \text{ Hz}^{-1}, \quad (1)$$

where  $m_{1.4\text{GHz}}$  is the reported magnitude,  $\alpha$  is the spectral index (i.e.,  $f(\nu) \propto \nu^{-\alpha}$ ), and  $D_L$  is the luminosity distance in cm as calculated from the redshift setting  $\Omega_m = 0.3$ ,  $\Omega_{\text{Lambda}} = 0.7$  and  $h = 0.7$ . We assumed  $\alpha = 0.7$ , which is intermediate of the typical range for radio jets (Bridle & Perley 1984). Our results do not qualitatively change if we assume either  $\alpha = 0.5$  or  $\alpha = 1.0$ .

According to Schneider et al. (2005), while only a small minority of FIRST-SDSS matches are chance superpositions, a significant fraction of the DR3 sources are extended radio sources. Therefore the FIRST catalog position for the latter may differ by more than  $2''$  from the optical position. To perform a comprehensive study of the BALQSO radio fraction, we built a full FIRST-SDSS cross-correlation catalog, containing all the detected radio components within  $30''$  of a optical quasar. In the following we used the Schneider et al. FIRST-SDSS catalog, but in § 3.2 we show that we obtain very similar results after extending the analysis to the full sample. In addition, many of the optical sources in SDSS are associated to more than one radio component in FIRST within  $30''$ , as expected if these sources are extended with jets and/or lobes separated from the central source. We will also discuss our results if we include the latter sources in the sample. When adopting the full FIRST-SDSS catalog, we used the integrated flux  $f_{\text{int}}$  listed in the FIRST catalog for each radio component and converted it to intrinsic radio luminosity using Eq. (1). When dealing with multiple sources we used the sum of the fluxes in the FIRST catalog.

Finally, we also stress that FIRST efficiently identifies radio matches to optically-selected quasars. By cross-correlating SDSS with the large radio NRAO VLA Sky Survey (Condon et al. 1998), Jiang et al. (2007) found in fact that only  $\sim 6\%$  of the matched quasars were not detected by FIRST. Most of these sources have offsets more than  $5''$  and are uniformly distributed in luminosity thus not altering the main conclusions of this paper.

### 3. RESULTS

#### 3.1. The Radio fraction of BALQSOs

The solid crosses in the left panel of Figure 1 show the fraction

$$f_{\text{BAL}} = \frac{N_{\text{BAL,RADIO}}}{N_{\text{RADIO}}}, \quad (2)$$

as a function of radio luminosity, where  $N_{\text{RADIO}}$  is the total number of radio quasars detected in SDSS and  $N_{\text{BAL,RADIO}}$  is the number of radio sources which are also classified as BALQSOs. For this plot we only used the “complete” SDSS optical

sample with apparent optical luminosities  $m_i \leq 19.1$ . The bins in  $L_{1.4\text{GHz}}$  were created adaptively starting from low radio luminosities by requiring a statistically significant sub-sample of least 25 quasars in defined as BALQSOs by the Trump et al. (2006) definition. In each bin we used the binomial theorem to estimate  $f_{\text{BAL}}$  along with its  $\pm 1\sigma$  confidence levels (e.g., Gehrels et al. 1986).

The first important result of our analysis is the high fraction of detected BALQSOs at low radio powers. The BALQSO fraction of  $45.5^{+7.6}_{-7.5}\%$  at the faintest radio powers of  $L_{1.4\text{GHz}} \lesssim 2 \times 10^{33} \text{ erg s}^{-1}$ , is significantly higher than that inferred from optical samples (e.g., Trump et al. 2006) and in strikingly good agreement with the 43% BALQSO occurrence inferred by DSS in the 2MASS-SDSS sample (shown with horizontal, thick-dotted lines in Figures 1 and 2). This result further supports and extends the key result discussed in DSS that the detected BALQSO fraction should be closer to the intrinsic one at longer wavelengths which are gradually less affected by dust absorption and extinction.

The second striking result of our study is that  $f_{\text{BAL}}$  drops rapidly with increasing radio power, rapidly dropping to  $31.2^{+6.0}_{-5.5}\%$  at  $L_{1.4\text{GHz}} \sim 3 \times 10^{33} \text{ erg s}^{-1}$  and down to  $23.9^{+3.4}_{-3.1}\%$  at  $L_{1.4\text{GHz}} \sim 7 \times 10^{33} \text{ erg s}^{-1}$ . This behavior strongly supports some close connection between radio and BALQSO phenomena and, as discussed below, poses serious challenges to simple evolutionary models. Using a sample of 29 BALQSOs, Becker et al. (2000) found the BALQSO fraction decreases for extremely radio-loud quasars. However, they found the trend was driven by the 11 low-ionization BALQSOs, whereas for the 18 high-ionization BALQSOs they were slightly under-represented at high radio loudness but not statistically significant. Using a much larger sample, we have confirmed the tentative trend detected by Becker et al. (2000) in the high-ionization BALQSOs.

#### 3.2. Robustness of Results

Our results are derived by cross-correlating optical quasars, RQs and BALQSOs. Therefore it is natural to expect that several issues may affect our results. In this section we carefully analyze all the most significant sources of bias which can enter our computations and find that none of these seems to be responsible for the observed  $f_{\text{BAL}} - L_{1.4\text{GHz}}$  behavior.

We first tested for biases from redshift or luminosity selection effects. By repeating our analysis using only the sources in two redshift bins  $1.7 \lesssim z \lesssim 2.5$  and, separately,  $2.5 \lesssim z \lesssim 4.38$ , we find very similar trends for the  $f_{\text{BAL}} - L_{1.4\text{GHz}}$  relation. The right panel of Figure 1 also shows the resulting  $f_{\text{BAL}}$  fraction for the Schneider et al. (2005) SDSS-FIRST sample with no optical magnitude cut. We again see a strong drop in the  $f_{\text{BAL}}$  fraction, by up to a factor of  $\sim 3$ . On the other hand our sample may suffer from selection effects in FIRST. At 3 mJy the completeness of FIRST is about 93%, decreasing to 75% at 1.5 mJy, and 55% at 1.1 mJy (see Figure 1 in Jiang et al. 2007). To check that our results were not affected by this incompleteness, we repeated our analysis to include only those sources with  $f_{\text{int}} > 3$  mJy. The strong observed drop in  $f_{\text{BAL}}$  remains unchanged.

As anticipated in § 2, the Schneider et al. (2005) cross-correlation sample is a *secure* identification of the core radio power associated to an optical quasar. However, to check for any bias in our results due to incomplete radio identifications in the SDSS DR3 quasar catalog, we recomputed  $f_{\text{BAL}}$  using the full sample built by matching SDSS and FIRST. The left

panel of Figure 2 shows the fraction of BALQSOs with optical luminosity brighter than  $m_i = 19.1$  for the sample using the total radio luminosity within  $5''$  of each optical source. When multiple components were present, we selected only the closest one to the central optical source. By widening the aperture from  $2''$  to  $5''$ , the number of quasars with radio identifications grows by about 27%. However, the strong drop in  $f_{\text{BAL}}$  at high radio powers is still present, meaning that fractions of sources are added to both the radio BALQSO and non-BALQSO samples. We found similar results when we included the sum of all radio sources within  $30''$ , as shown in the right panel of Figure 2, although some additional noise is present in this case.

The dashed crosses in both Figures 1 and 2 show  $f_{\text{BAL}}$  as a function of radio luminosity if we adopt the original, more stringent, classification by Weymann et al. (1991). Although the fraction of BALQSOs inevitably decreases by about a factor of 2, we still find a statistically significant, and even stronger, decrease in  $f_{\text{BAL}}$  by up to a factor of  $\sim 10$  at  $L_{1.4\text{GHz}} \gtrsim 2 \times 10^{34} \text{ erg s}^{-1}$ . The value of  $f_{\text{BAL}}$  at low radio powers again agrees with the simulations by DSS that argued for an intrinsic fraction of  $\sim 20\%$  for BALQSOs based on the BI classification (shown with horizontal, thin-dotted lines in Figures 1 and 2). For the rest of the paper we focus on the result using the Trump et al. (2006) definition of BALQSOs, although we will discuss results from the alternative BI classification where relevant.

In Figure 3 we show the distributions of BALQSOs (red-dashed lines) and non-BALQSOs (black-solid lines) as a function of radio luminosity for different bins of optical luminosity. These bins were chosen to provide an equal number of BALQSOs in each panel. It is apparent that unlike the BALQSOs, the non-BALQSO distributions have a greater tendency to populate significantly higher radio luminosity bins. This provides more evidence that the trends in  $f_{\text{BAL}}$  are not a mere consequence of random effects in the radio power distributions of optical quasars.

We conclude that the behavior of  $f_{\text{BAL}}$  as a function of radio power seems to be an intrinsic, real feature of the RQ population, not linked to any significant selection effect or specific type of radio identification considered.

#### 4. EXPLAINING THE OBSERVED TREND

Models aimed at explaining the BALQSO and/or radio fractions, can be broadly divided into two extreme scenarios: one in which each quasar phase is distinct and characterized by the internal physical *evolution* undergone by the system, and the other in which all these phenomena co-exist at all times but different source *orientation* modify the observed balance of one process with respect to another.

##### 4.1. The Evolutionary Model

The results discussed in § 3 seem to pose a serious challenge to “evolutionary” models for BALQSOs. The simple sketch shown in the left panel of Figure 4, represents the basic picture for the evolution of a black hole within its host galaxy (e.g., Kawakatu et al. 2003). The mass of the central black hole, shown as a solid line in the left panel of Figure 4, exponentially grows through gas accretion from the surrounding medium. Initially the whole galaxy, or at least its central region, is buried under optically-thick layers of dust which allow the AGN to be detectable only in those bands which suffer less from obscuration, such as in X-rays (e.g., Ueda et al. 2003). When

the black hole becomes sufficiently luminous, it injects enough energy and momentum (e.g., Fabian 1999) into the surrounding medium to disperse the obscuring material. During this blowout phase, the system will be detected as a BALQSO featuring the signatures of strong winds in their spectra, while at later stages it will be observed as an optical, dust-free quasar.

It is still unclear what triggers the radio activity of an AGN (e.g., Sikora et al. 2007), so it is difficult to predict when an optical quasar should become radio-loud (e.g., Shankar et al. 2007b). Nevertheless, in pure evolutionary models the radio phase is usually viewed as a brief period within the optical phase as the incidence of RQs in optical samples is rather small, ( $\sim 15\text{--}20\%$ , e.g., Jiang et al. 2007; see also § 1). In this model, our results on  $f_{\text{BAL}}$  indicate that the radio duty cycle must overlap the boundary between the BALQSO and optical phases, because a significant fraction of optical quasars also emit in radio but are not BALQSOs, and vice versa.

In a pure evolutionary model our result that  $f_{\text{BAL}} \sim 45\%$  constrains the BAL and non-BAL phases to last for a similar time within the brief radio phase, which is about  $15\text{--}20\%$  of the total optical quasar lifetime (see left panel of Figure 4). However, this model requires a great deal of fine tuning to explain the fast drop in  $f_{\text{BAL}}$  at high radio powers. A simple explanation for such a trend may be an increasing feedback efficiency with quasar luminosity (e.g., Kelly et al. 2008). The more luminous sources would then be faster in removing the surrounding obscuring medium, shortening the BALQSO phase and consequently inducing a decrease in  $f_{\text{BAL}}$ . However, this model is at variance with the results by DSS who found the BALQSO fraction to be constant with optical luminosity among the most luminous quasars.

##### 4.2. The Orientation-Beaming Model

We propose that a simple orientation effect can fully explain the puzzling trend in the  $f_{\text{BAL}}\text{--}L_{1.4\text{GHz}}$  distribution. We posit that some fraction of RQs are relativistically beamed towards the observer and are boosted to higher radio luminosities. Since the radio luminosity function is steep, beamed radio sources are a disproportionate fraction of the bright sources. Following disk wind models (e.g., Murray et al. 1995, Proga et al. 2000), we then assume that radio BALQSOs must be non-beamed sources, preferentially viewed close to the plane of the accretion disk surrounding the central black hole. It is then reasonable to expect that if BALQSOs are a fixed fraction of the *intrinsic* radio luminosity function, then the observed occurrence of BALQSOs must decrease at high radio powers due to the apparent increase of  $N_{\text{RADIO}}$  in Eq. (2) towards high luminosities due to beaming.

We quantitatively explore this basic idea by building a simple “unification” model (e.g., Urry & Padovani 1995). The intrinsic radio quasar luminosity function was assumed to be a power-law  $\Phi(L_R) \propto L_R^{-\beta}$  with arbitrary normalization and slope  $\beta = -2.75$ , which is an average of the bright-end slopes measured for the optical and radio quasar luminosity functions (e.g., De Zotti et al. 2005, Richards et al. 2006, Jiang et al. 2006)<sup>2</sup>. We then assumed that the population of radio quasars is composed of three sub-populations, as sketched in the right panel of Figure 4. The first one is represented by radio BALQSOs, which are preferentially viewed at lines of sight close to the disk or the torus, at a maximum angle of  $\theta \lesssim 25^\circ$ , corresponding to a fraction of  $\sin(\theta) = 43\%$ , as inferred by DSS. Following

<sup>2</sup> The exact value of this slope does not affect our results as the uncertainties in this parameter are degenerate with the uncertainties in other model parameters

Urry & Padovani (1995) we then assumed that the fraction of beamed sources is viewed at an angle of  $38^\circ$  from the jet axis, corresponding to a fraction of  $\sim 21\%$ . The last sub-group is composed of radio non-beamed sources viewed at intermediate angles accounting for the remaining 36% of the total. The relative contributions of the different type of sources to the total radio luminosity function are shown in the left panel of Figure 5, in units of  $L^3 \Phi(L)$  to enhance the difference among the lines.

The luminosity function of beamed sources was computed following the method outlined in Urry & Padovani (1991). The observed luminosity function at a given observed luminosity  $L_{\text{obs}}$  was obtained by convolving the intrinsic luminosity function with the probability  $P(L_{\text{obs}}|L_{\text{int}})$ . Following Urry & Padovani (1991) we allowed beamed sources to also have a diffuse component from the lobes and the core, in addition to the beamed emission. Therefore the observed luminosity of this sub-group was parameterized as  $L_{\text{obs}} = (1 + f\delta^p)L_{\text{int}}$ , where  $L_{\text{int}}$  is the intrinsic luminosity,  $f$  is the fraction of luminosity in the jets,  $\delta = [\gamma(1 - \beta \cos \theta)]^{-1}$  is the Doppler factor corresponding to a given angle  $\theta$  and Lorentz factor  $\gamma = (1 - \beta^2)^{-1/2}$ , and the exponent  $p$  is a parameter depending on the spectrum and reacceleration of the radiating particles. Given the relatively high number of parameters in this model, we adopt  $p = 3$ ,  $\gamma = 11$ ,  $f = 0.005$  and the maximum beaming angle to  $\theta_{\text{max}} = 38^\circ$ . These are the same values used by Urry & Padovani (1995) and, more recently, by Padovani et al. (2007) to reproduce within unification models the luminosity distributions of samples dominated by beamed sources.

The apparent luminosity function of beamed radio sources, “crosses” the intrinsic luminosity function at a luminosity which depends on the minimum luminosity in which we allow beamed sources to appear in the luminosity function (see Figure 5). We parameterized this luminosity as  $\log L_{\text{MIN}} = 32 - \Delta \log L$ , where  $L_{1.4\text{GHz}} \sim 10^{32} \text{ erg s}^{-1}$  is the minimum luminosity in the sample. The solid line in the right panel of Figure 5 shows our best-fit model for the expected fraction of BALQSOs as a function of radio luminosity. Optimizing the model to the  $L_{1.4\text{GHz}}$ -dependence of  $f_{\text{BAL}}$ , we find  $\Delta \log L = 0.094^{+0.016}_{-0.014}$ , with  $\chi^2_{\text{min}} \sim 4.1$ , for 7 degrees of freedom. This model implies that beamed sources are almost absent in the luminosity function below  $L_{1.4\text{GHz}} \sim 10^{32} \text{ erg s}^{-1}$  and then start to become important only above this luminosity threshold. To better compare with the data, we also show with open circles the expected fraction for this model integrated over the same radio luminosity bins of the data.

In this model the dependence of the BALQSO fraction on radio luminosity is entirely due to geometry and it is independent of the duty cycle of RQs within the overall quasar population. Nevertheless, the origin of the radio emission can still be an evolutionary phase or related to specific properties of quasars such as the magnetic field, the black hole mass, spin or Eddington ratio. Irrespective of the specific model considered, the non-trivial dependence of the BALQSO fraction on radio luminosity found in this paper indicates the RQ and BALQSO phenomena are related.

#### 4.3. The Energy Exchange Model

Another possible explanation for the drop in  $f_{\text{BAL}}$ , could rely on some sort of rest-mass “energy exchange” from the wind to the jet in high luminosity radio sources. Within the framework of the geometrical model, the energy gained by the system from the external gas accretion rate must be redistributed between the jet and the wind by some physical mechanism, such as the mag-

netic field. We could then expect that those quasars with high radio powers preferentially inject energy into the jet due to a stronger intrinsic magnetic field and/or a rapidly spinning central black hole, thus limiting the energy channeled into the wind and inevitably causing a drop in  $f_{\text{BAL}}$ .

In Figure 6 we tested this idea by plotting, as proxies of the wind power, the BALQSO absorption index, AI (upper panel), and the maximum velocity  $V_{\text{max}}$  (lower panel) measured from the absorption troughs, as a function of radio luminosity. In each bin, the quantities were computed from the biweight-mean (Hoaglin et al. 1983) and the errors on this mean are estimated from the biweight- $\sigma$  reduced by  $\sqrt{N}$ , where  $N$  is the number of BALQSOs in the bin. The significant decrease in AI with radio power could be simply viewed as a decrease in the amount of obscuring mass for the more luminous sources. This is consistent with Becker et al. (2000), who found BI decreases with radio luminosity for the high-ionization BALQSOs. The wind velocity instead is independent of  $L_{1.4\text{GHz}}$ , although with a large scatter. This suggests that there is no decrease in the wind speed at high radio powers. This alternative model may also conflict with evidence that AGNs have similar radiative and kinetic efficiencies (e.g., Shankar et al. 2007a,b). Moreover, if the efficiency is constant, then  $V_{\text{max}}$  should increase with luminosity (i.e. with the mean accretion rate), rendering the result on its flatness rather intriguing (e.g., Ganguly et al. 2007). We will explore these issues in future work.

## 5. CONCLUSIONS

We found that the fraction of BALQSOs among the FIRST radio selected sources in the SDSS DR3, is about 45% at faint radio powers, significantly higher than that measured in the optical but consistent with that inferred by DSS from infrared selected quasars, but then drops by a factor of  $\gtrsim 2$  at  $L_{1.4\text{GHz}} \sim 2 \times 10^{33} \text{ erg s}^{-1}$ . The magnitude of the fractional drop does not depend on the definition of BALQSO. The detected fraction at low radio luminosities is consistent with the recent estimate of 43% inferred in infrared bands by DSS, supporting the fact that longer, less absorbed wavelengths, are more suitable for probing the intrinsic fraction of BALQSOs. We therefore agree with Hewett and Foltz (2003) who claimed a similar occurrence of BALQSOs in optical and radio samples, although our results are supported by a much larger sample. The variation of the BALQSO fraction with radio power is similar to that found by Becker et al. (2000) and Hewett and Foltz (2003), but with our much larger sample we have been able to measure the dependence. We checked that the decrease in the number of radio BALQSOs is real, in the sense that it is not dependent on redshift or luminosity cuts, biased by optical or radio selection effects, or dependent on the specific type of radio source considered (core-dominated or extended with multiple components). We also found that at fixed optical magnitude, the highest bins of radio luminosity are preferentially populated by non-BALQSOs rather than BALQSOs. These results are difficult to reconcile with a strictly evolutionary model for BALQSOs, but they fit well within a simple orientation-based model where the apparent radio luminosity function is made by a superposition of beamed and non-beamed radio sources in which BALQSOs are non-beamed radio sources preferentially viewed at large angles, close to the plane of the disk.

We acknowledge discussion at the AGN lunch in the OSU astronomy department. We thank Chris Kochanek for helpful comments that improved the presentation of this work.

## REFERENCES

- Becker, R. H., White, R. L., & Helfand, D. J. 1995, *ApJ*, 450, 559
- Becker, R. H., White, R. L., Gregg, M. D., Brotherton, M. S., Laurent-Muehleisen, S. A., & Arav, N. 2000, *ApJ*, 538, 72
- Bridle, A. H., & Perley, R. A. 1984, *ARA&A*, 22, 319
- Condon, J. J., et al. 1998, *AJ*, 115, 1693
- Croton, D. J., Springel, V., White, S. D. M., De Lucia, G., Frenk, C. S., Gao, L., Jenkins, A., Kauffmann, G., Navarro, J. F., & Yoshida, N. 2006, *MNRAS*, 365, 11
- Dai, X., Shankar, F., & Sivakoff, G. R. 2007, *ApJ*, accepted, arXiv:0704.2882
- De Zotti, G., Ricci, R., Mesa, D., Silva, L., Mazzotta, P., Toffolatti, L., & González-Nuevo, J. 2005, *A&A*, 431, 893
- Fabian, A. C. 1999, *MNRAS*, 308, 39
- Ganguly, R., Brotherton, M. S., Cales, S., Scoggins, B., Shang, Z., & Vestergaard, M. 2007, *ApJ*, 665, 990
- Gehrels, N. 1986, *ApJ*, 303, 336
- Granato, G. L., Silva, L., Lapi, A., Shankar, F., De Zotti, G., Danese, L. 2006, *MNRAS*, 368L, 72
- Hewett, P. C., & Foltz, C. B. 2003, *AJ*, 125, 1784
- Hoaglin, D. C., Mosteller, F., & Tukey, J. W. 1983, in “Understanding robust and exploratory data analysis”, Wiley Series in Probability and Mathematical Statistics, New York: Wiley, 1983, edited by Hoaglin, D. C., Mosteller, F., & Tukey, J. W.
- Hopkins, P. F., Hernquist, L., Cox, T. J., Di Matteo, T., Robertson, B., & Springel, V. 2006, *ApJS*, 163, 1
- Jiang, L., Fan, X., Ivezić, Ž., Richards, G. T.; Schneider, D. P., Strauss, M. A., & Kelly, B. C. 2007, *ApJ*, 656, 680
- Kawakatu, N., Umemura, M., & Mori, M. 2003, *ApJ*, 583, 85
- Kellermann, K. I., et al. 1989, *AJ*, 98, 1195
- Kelly, B. C., Bechtold, J., Trump, J. R., Vestergaard, M., & Siemiginowska, A. 2008, *ApJ*, accepted, arXiv:08012383
- King, A. 2003, *ApJ*, 596, L27
- Lapi, A., Shankar, F., Mao, J., Granato, G. L., Silva, L., De Zotti, G., & Danese, L. 2006, *ApJ*, 650, 42
- Matthews, T. A., & Sandage, A. R. 1963, *ApJ*, 138, 30
- Murray, N., Chiang, J., Grossman, S. A., & Voit, G. M. 1995, *ApJ*, 451, 498
- Padovani, P., Giommi, P., Landt, H., & Perlman, E. S. 2007, *ApJ*, 662, 182
- Richards, G. T., et al. 2006, *AJ*, 131, 2766
- Schmidt, M. 1963, *Nature*, 197, 1040
- Schneider, D. P., et al. 2005, *AJ*, 130, 367
- Shankar, F., Lapi, A., Salucci, P., De Zotti, G., & Danese, L. 2006, *ApJ*, 643, 14
- Shankar, F., Weinberg, D. H., & Miralda-Escudé, J. 2007a, *ApJ*, submitted , arXiv/0710.4488
- Shankar, F., Cavaliere, A., Cirasuolo, M., & Maraschi, L. 2007b, *ApJ*, accepted
- Sikora, M., Stawarz, L., & Lasota, J.-P. 2007, *ApJ*, 658, 815
- Stoeke, J. T., Morris, S. L., Weymann, R. J., & Foltz, C. B. 1992, *ApJ*, 396, 487
- Trump, J. R., et al. 2006, *ApJS*, 165, 1
- Ueda, Y., Akiyama, M., Ohta, K., & Miyaji, T. 2003, *ApJ*, 598, 886 (U03)
- Urry, M., Padovani, P. 1991, *ApJ*, 371, 60
- Urry, M., Padovani, P. 1995, *PASP*, 107, 803
- Weymann, R. J., Morris, S. L., Foltz, C. B., & Hewett, P. C. 1991, *ApJ*, 373, 23

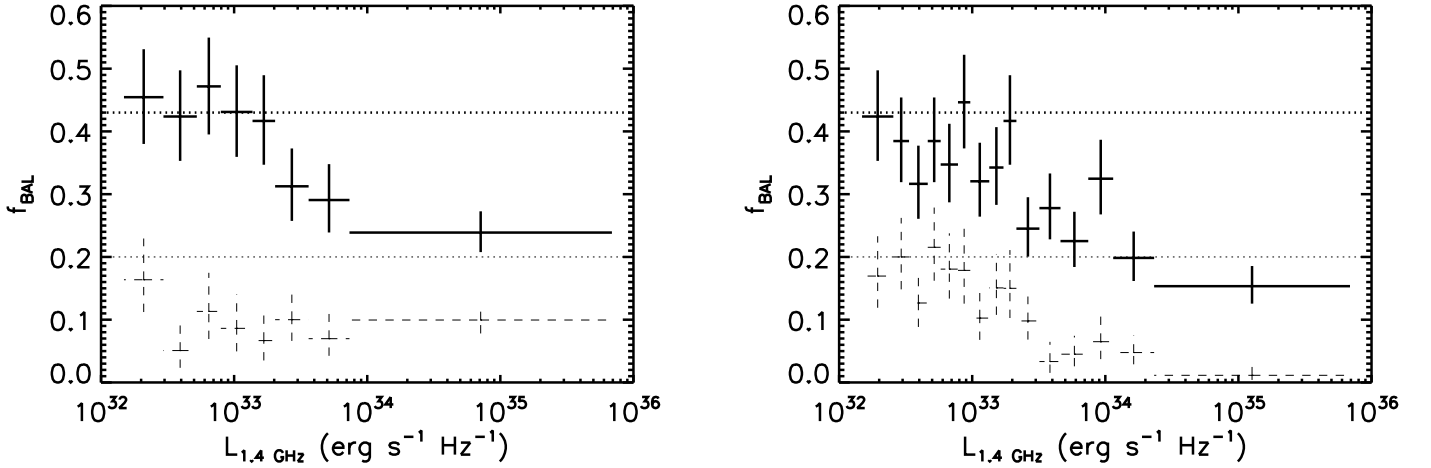


FIG. 1.— *Left panel*: the crosses show the fraction of BALQSOs within the radio sample of the total SDSS quasars with optical luminosity brighter than  $m_i = 19.1$  averaged over bins of radio luminosity, from the  $2''$  cross-correlation sample of Schneider et al. (2005); the dashed crosses show the same binning for the BALQSOs sample built following the more restrictive definition of Weymann et al. (1991) for BALQSOs; the thick and thin-dotted lines refer to the “intrinsic fraction” of 43% and 20% of BALQSOs found in 2MASS by Dai et al. (2007), following the Trump et al.’s (2006) and Weymann et al. (1991)’s definitions, respectively. *Right panel*: fraction of BALQSOs within the whole SDSS sample of RQs; here all lines and symbols are as in the left panel; the statistical significance of the drop in the radio-BALQSOs fraction towards high powers is now evident also for the BALQSO sample built on Weymann et al.’s definition.

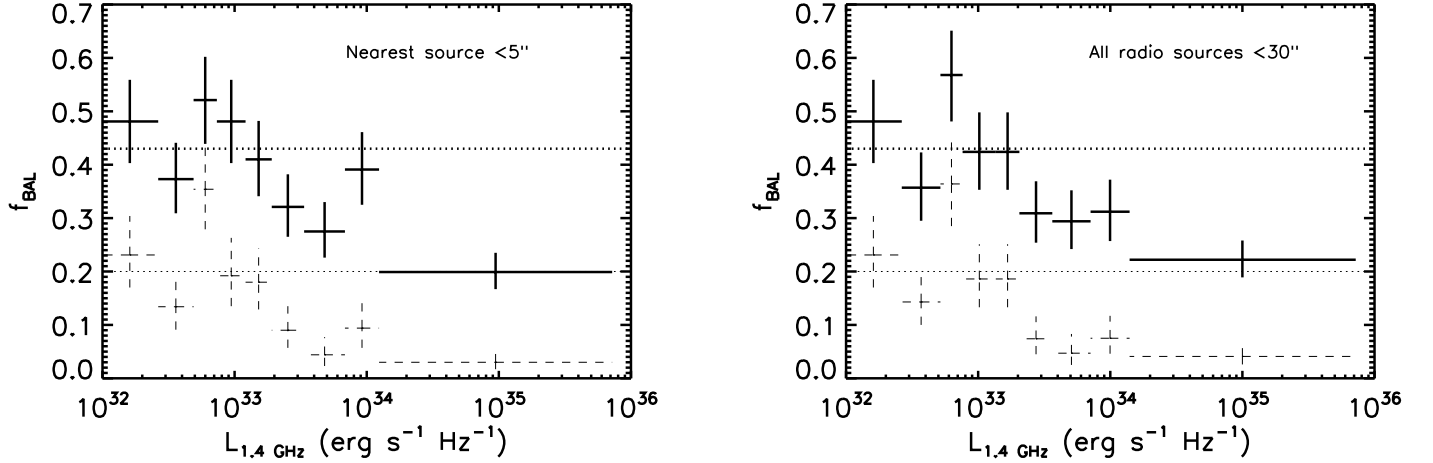


FIG. 2.— Fraction of BALQSOs with an optical flux brighter than  $m_i = 19.1$  within the radio sample derived from the full FIRST-SDSS cross-correlation. The lines and symbols are as in Figure 1. Given the sensible increase in sample statistics in this case, our adaptive binning method produces several extra bins in the  $f_{\text{BAL}}-L_{1.4 \text{ GHz}}$  distribution. *Left panel:* the crosses show the fraction of BALQSOs within the radio sample defined for sources which lie within  $5''$  of the optical source; if multiple radio components are contained within this aperture, then only the closest source is considered. *Right panel:* here the crosses show the fraction of BALQSOs within the radio sample defined for sources which lie within  $30''$  of the optical source; if multiple radio components are present within this aperture, then they are treated as a single source with radio power given by the sum of the integrated flux of each component. In both panels the dashed crosses show the results adopting the Weymann et al. (1991) definition of a BALQSO.

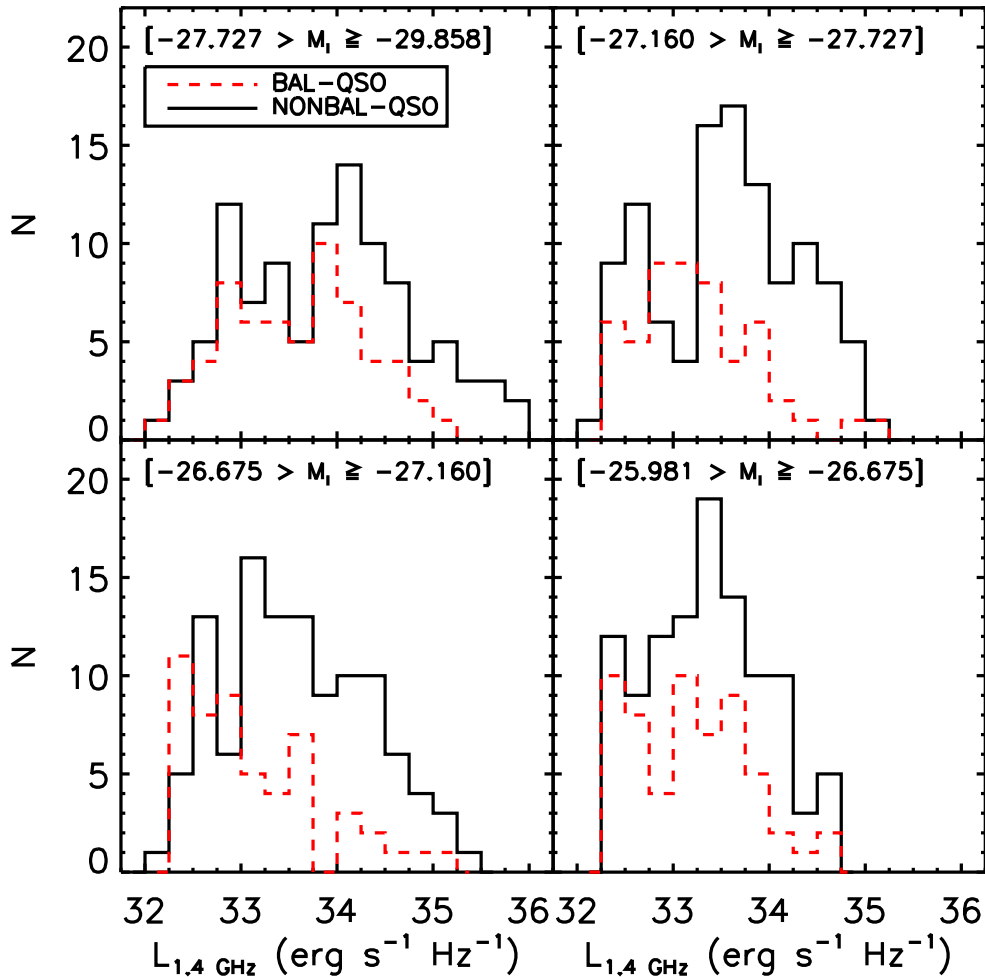


FIG. 3.— The dashed and solid lines show, respectively, histogram of the distributions of BALQSOs and non-BALQSOs as a function of radio luminosity in different bins of optical luminosity. Unlike the BALQSOs, the non-BALQSOs have a greater tendency to form a prolonged tail of very luminous, potentially beamed, radio sources.



FIG. 4.— *Left panel*: schematic diagram of a pure “evolutionary” model. The mass of the central black hole starts growing in a heavily obscured phase. When it becomes sufficiently luminous to blow away the surrounding medium, it can then be detected as a BALQSO and then finally as an optical, dust-free quasar. *Right panel*: schematic representation of a simple “orientation” model for RQs and BALQSOs. The radio phase in both schemes is always considered as a brief period within the optical phase.

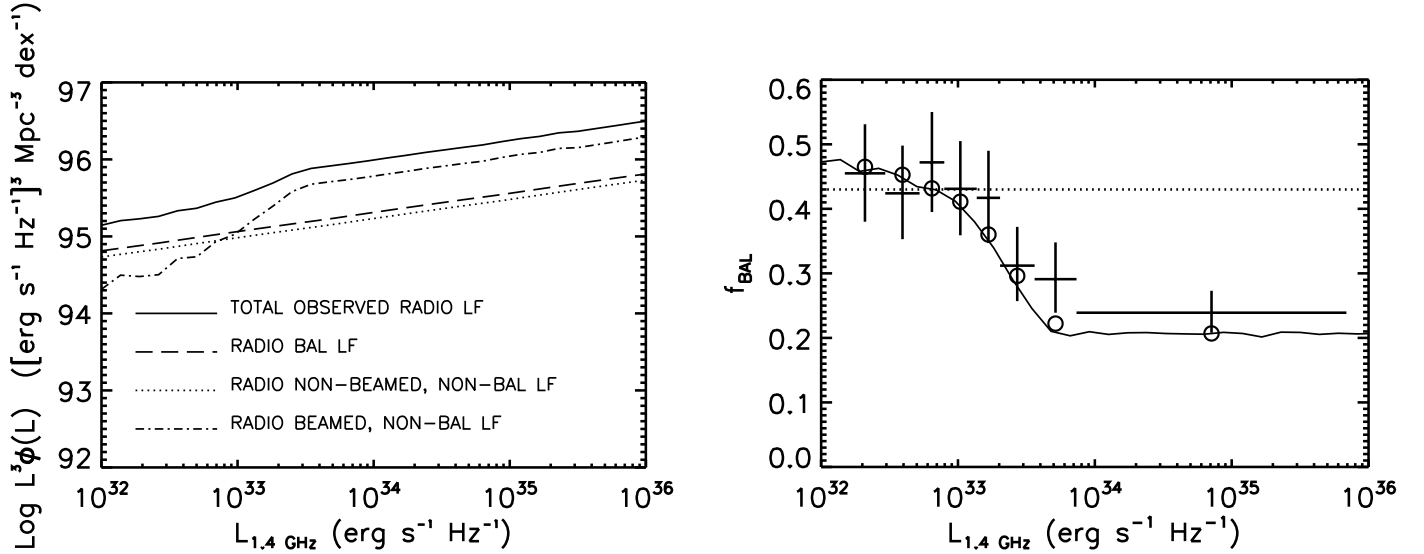


FIG. 5.— *Left panel*: radio quasar luminosity functions plotted in units of  $L^3 \Phi(L)$  to enhance the differences; the *long-dashed* line is the luminosity function of RQs detected as BALQSOs, normalized to be 43% the one of the intrinsic total radio quasar luminosity function, and an identical slope of  $-2.75$ ; the *dotted* line is the fraction of  $\sim 0.21\%$  of radio non-beamed sources, while the *dot-dashed* line is the fraction of  $\sim 0.36\%$  of beamed sources (see text for details); the *solid* line is the total apparent luminosity function for all radio quasars which would be observed for this model. *Right panel*: the *solid* line represents the expected fraction of BALQSOs as a function of radio luminosity, derived as the ratio of the *dashed* and *solid* lines in the left panel; the *open circles* show the expected fraction averaged over the same radio luminosity bin as the data; all other symbols and lines are as in the left panel of Figure 1.

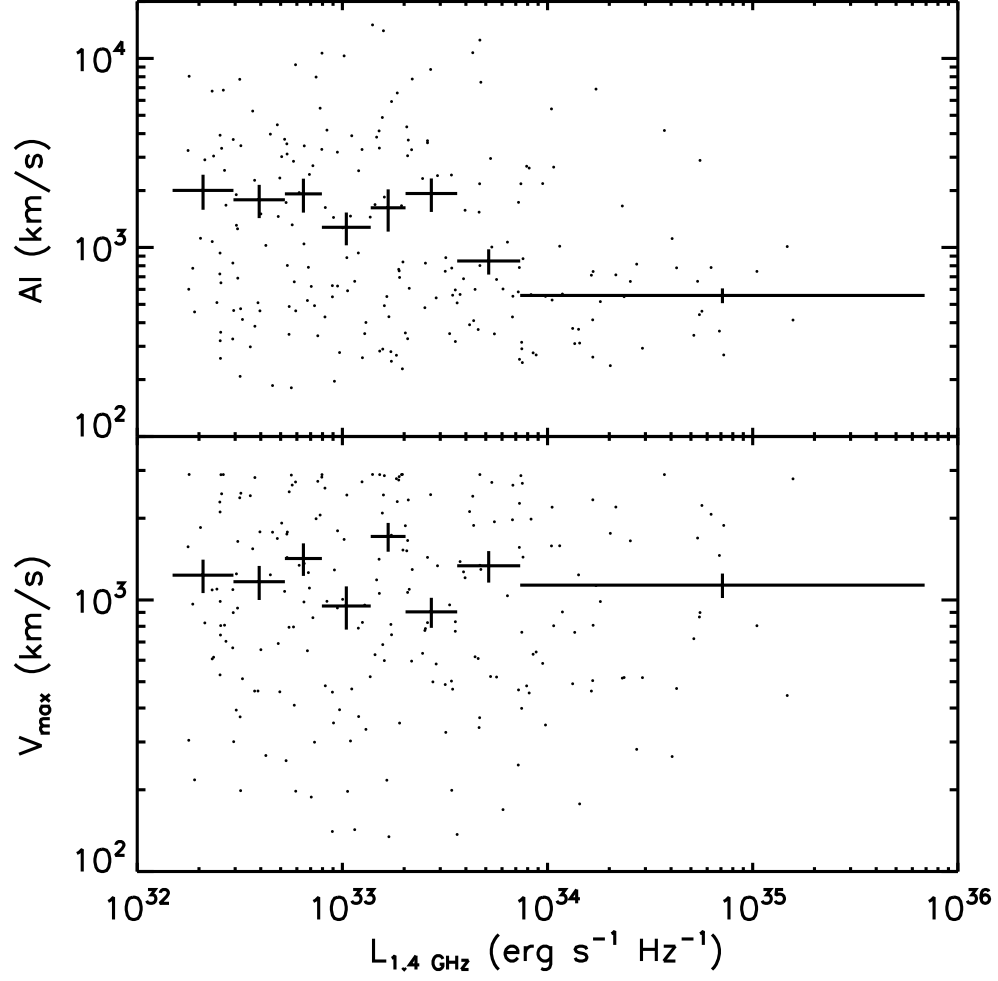


FIG. 6.— *Upper panel:* BALQSO Absorption Index per bin of radio luminosity shown with *crosses*; also shown the full sample with *solid points*. *Lower panel:* maximum velocity measured from the absorption troughs as a function of radio luminosity; a very similar, constant, behavior is obtained by plotting the weighted average velocity of the BALQSOs troughs. We do not find any significant evidence for the wind velocity to decrease with increasing radio luminosity.